Bio-based composites made from bamboo fibers with high lignin contents: a multiscale analysis

Cécile Sillard, Eder Castro, Jerachard Kaima, Quentin Charlier, Jérémie Viguié, Maxime Terrien, Ittichai Preechawuttipong, Robert Peyroux, Evelyne Mauret, Alain Dufresne

Bio-based composites made from bamboo fibers with high lignin contents: a multiscale analysis

Cécile. Sillard [a*], Eder Castro[a], Jerachard. Kaima[b,c], Quentin. Charlier[a], Jérémie Viguié[a], Maxime Terrien[a], Ittichai. Preechawuttipong[c], Robert. Peyroux[b], Evelyne Mauret[a], Alain Dufresne[a]

[a] Université Grenoble Alpes, Grenoble INP, CNRS UMR 5518, LGP2, 38000 Grenoble, France

[b] Université Grenoble Alpes, Grenoble INP, CNRS UMR 5521, 3SR, 38000 Grenoble, France

[c] Department of Mechanical Engineering, Faculty of Engineering, Chiang Mai University, Chiang Mai, Thailand

* Corresponding Author: cecile.sillard@lgp2.grenoble-inp.fr

Abstract

To meet societal and economic expectations, the bio-based composites market is developing. However, some issues remain, especially for lignocellulosic fiber composites, due to their highly hydrophilic nature which impacts the composite performance. This study focuses on bamboo fiber-polypropylene composites manufactured by film stacking using fiber mats obtained through a wet laid process. To individualize fibers, raw bamboo was cooked using a soda treatment in order to keep a certain amount of lignin on fiber surface. A maximum surface lignin content of 81.%, measured by XPS analysis, was obtained, from the 1 wt.% soda treatment. The corresponding bulk lignin content, measured by Klayson method, is 21.%. The macroscopic properties of bamboo fiber-polypropylene composites were evaluated in regard of material microstructure through a multiscale analysis. The best mechanical properties were obtained for composites manufactured from bamboo fiber prepared using a 1 wt.% soda treatment, which corresponds to the highest lignin content (3,5 GPa and 53 MPa for modulus and strength in tensile tests, 3,8 GPa and 64 MPa in bending tests). The good mechanical performance of the composites was attributed to the improved compatibility between the fiber and the matrix, evidenced by multiscale studies.

Keywords: Bio-composites; Natural fibers; Interface/interphase; Mechanical testing; Atomic force microscopy.

1. Introduction

Since the last decade, the interest in using bio-based composites as an alternative to petroleum-based materials has rapidly increased. This topic has already been actively investigated and reviewed in the scientific literature for the large panel of existing natural fibers as filler and/or reinforcement [1,2]. These materials can achieve a wide range of properties (from high stiffness to low density for high strength-to-weight ratio) while answering societal and economic expectations (it is possible to design low cost and partially or fully biodegradable solutions, and so on.) [3]. The global market for bio-composites was 16.46 USD billion in 2016 and is projected to reach 36.76 billion by 2022 [4].

The main natural fibers used in composite applications are extracted from flax, hemp, kenaf, or sisal [5]. However, Gu et al. [6] proved that bamboo fibers (BF) could replace flax for the development of bio-based composites. BF market has increased over the last decade due to the fast growth of bamboo (3 years to reach adult form), its low cost (around 0.5-0.6 €/kg, compared to 3.11 €/kg for flax and 2€/kg for glass fibers) and broad availability [7-9]. According to the Food and Agriculture Organization and the International Bamboo and Rattan Organization, bamboo covers over 37 million hectares worldwide, mainly in Asia and South America. Furthermore, bamboo has notable intrinsic properties such as a high stiffness due to high lignin contents (around 30.% for some species) which makes them interesting candidates for reinforcing components in bio-based composites [7, 10, 11].

However, the use of natural fibers in composites is still challenging, especially due to the lack of compatibility between hydrophilic fibers and polymer matrices that are generally hydrophobic. Different solutions have been proposed to improve this compatibility through physical, physico-chemical or mechanical methods to modify the wettability or the roughness of fibers (such as ultrasonic or corona treatment) [9]. Bio-inspired strategies relying on the adsorption of nano-objects at the surface of fibers to increase their roughness and specific

surface have also been used [12, 13]. Another solution to improve compatibility is to create covalent bonding between matrix and fibers by adding reactive groups at the surface of the fiber or inside the polymer matrix. The most known methods for natural fiber modification consider grafting hydrophobic compounds such as isocyanates, acid anhydrides or silanes on the fiber surface [14-16]. The polymer matrix can be also modified, for example through the addition of maleic anhydride. It has been shown that chemical grafting in general increases the stiffness of the composite but it is expensive and not eco-friendly.

Before being able to obtain composites, raw biomass must be converted to obtained natural fillers or fibers. A lot of methods exist, leading to a wide range of products, from macro-pellets to nano-fibrils. For instance, soda cooking is a simple process which produces individual fibers at micro-scale without damaging too much their structure. The best-known chemical cooking to prepare natural fibers is soda treatment, which produces individual fibers by removing hemicelluloses and a part of the lignin at low temperature, while retaining the majority of cellulose [17]. Soda cooking to obtain BF has been well studied. The influence of soda concentration and reaction time on single fiber properties have been reported [19], showing the influence of the NaOH concentration and the reaction time for three types of bamboo fibers. For severe soda treatment, natural fibers became more ductile [20,21, 22] than without any treatment. It was also reported that interfacial adhesion between fiber and matrix and composite ultimate strength can be improved using alkali treatments [18]. Nevertheless, to our knowledge, the correlation between lignin content and mechanical properties of natural fiber composites has not been investigated so far. Our hypothesis is that the lignin content, and in particular the amount of lignin available at the surface of natural fibers, could lead to a better compatibilization with non-polar matrices, and thus to bio-based composites with improved properties.

Furthermore, the preparation of the mat following fiber individualization, which is generally barely reported, should be better controlled or optimize, to increase the amount of fiber specific surface available. This could explain in part why the literature is composed by a large amount of

different results regarding the mechanical properties of bio-based composites prepared using close conditions.

In this context, the objectives of this study are to obtain homogenous BF-polypropylene (PP) composites while maintaining a certain amount of lignin at the surface of BF in order to improve the compatibility between both components. To reach such a goal, BF were individualized using soda treatment with various soda concentrations and BF mats were obtained through a wet laid approach inspired from papermaking processes. BF-PP composites were then manufactured by hot-pressing film stacking.

BF bulk and surface lignin content were estimated using X-ray Photoelectron Spectroscopy (XPS) analysis and Klason method. Atomic force measurement (AFM) was used to measure the fiber surface roughness means square (RMS) at nanoscale and the adhesion between BF and polyethylene (PE) beads. The mechanical behavior of BF-PP composites was analyzed in both static and dynamic modes using dynamic mechanical analysis (DMA) and tensile and flexural tests.

2. Experimental section

2.1 Materials

The middle internode part of a grand bamboo (*Dendrocalamus elegans*) older than three years, from Mok Far Mont Ngo Resort, Chiang Mai, Thailand, was used as raw material. The bamboo was first cut into small strips of 1 mm × 5 mm × 60 mm, dried in ambient conditions for 7 days, and then stored in plastic bags.

30.% bio-based polypropylene pellets were supplied by Natureplast (reference NP BioPP 202-48). Technical datasheets indicate a density of 0.9 g.cm^{-3}, a tensile modulus of 1.25 GPa, a Vicat temperature of 151.°C, and a heat distortion temperature (HDT) of 92.°C.

NaOH 99.% used for soda treatment was supplied by Roth Sochiel.

2.2 Fiber preparation by soda treatment

Bamboo strips were dried for 24h in an oven at 105ºC before cooking. To perform the soda treatment, strips are mixed in a soda solution and introduced in a multi-shell reactor ERTAM.

The suspension is then heated at 120.°C for 120 min at 1-2 bars with a temperature ramp at 4.°C/min. The multi-shell reactor consists of six stainless steel autoclaves with a capacity of 3.3 L placed in an oil bath. The device rotates during the cooking to ensure a good mixing. The soda treatment was performed at different concentrations of soda (1, 6, and 30 wt.%) for a bamboo/solution weight ratio of 1/12.

2.3 Fiber characterization

MorFi analysis. The morphology of BF was characterized using a MorFi device (Techpap, France) which consists in the image analysis of micrographs taken by optical microscopy of fiber suspensions. 300 mg of BF were diluted in 2 L of water and kept under constant circulation during the image acquisition. The fiber/fine limit was set at 200 μm in length, and the analysis was carried out until 30,000 fibers were detected. The analysis was performed three times on each sample, and the average fiber length and width were determined.

Bulk lignin content. Soluble and insoluble lignin contents were measured by the Klason method following the Tappi T 222 om-11 and Tappi UM 250 standards. 1 g of fibers previously dried overnight at 105 .°C was added to 15 mL of sulfuric acid solution at 72.%. The mixture was then stirred for 2 h, diluted with water to get 575 mL of 3.% acid solution, and boiled for 4 h. The mixture was finally filtered and the mass of solid content was measured after having been dried for 24 h at 105.°C. The soluble lignin content was measured by ultraviolet spectroscopy at $\lambda = 205$ nm.

Crystallinity index. The crystallinity index was measured by X-ray diffraction (XRD) analysis using an X'Pert Pro MPD diffractometer PANALYTICAL (Netherlands) equipped with a Bragg-Brentano geometry and a copper Kα anode ($\lambda = 0.1542$ nm). Crystallinity indices were obtained by subtracting the amorphous contribution from the diffraction profile as shown in Fig. 1 [23,24]. XRD was carried out on a zero-background Si substrate. An amorphous reference (in powder form) was produced by cryocrushing 1 g of raw eucalyptus fibers for 20 min at 30 Hz

with 2 zirconium balls in a 20 mL chamber cooled with liquid nitrogen. The 2Θ diffraction angle ranged from 6° to 60° with a 0.05° interval.

Fig. 1.

Scanning electron microscopy (SEM). SEM images were obtained using a FEI QUANTA 200 SEM (USA) at 10 keV. Samples were coated with gold using a rotary pumped coater Q150OR ES plus (Quorum) prior to observation.

Calculation of surface lignin content. Surface lignin content was evaluated by X-ray Photoelectron Spectroscopy (XPS) analysis using a K, ALPHA THERMOFISHER (USA). Measurements were performed using a Kα apparatus modulated with a monochromatic Al Kα X-ray source at 14,875 eV. Mat samples were positioned perpendicularly to the source under ultrahigh vacuum (below 10^{-7} Pa). Spectra patterns were decomposed using Advantage software. The O/C ratio, which represents the number of oxygen (O) atoms per carbon (C) atom at the surface, was calculated using (Eq.1).

$$O/C = (Io/So) * (Sc/Ic) \qquad \text{(Eq. 1)}$$

where I_O and I_C are the intensity of the oxygen and carbon peaks, respectively, and S_C and S_O are equal to 0.00170 and 0.00477 for carbon and oxygen, respectively. The theoretical surface lignin content can then be estimated form the O/C values for pulp sample, lignin free pulp, and lignin using (Eq. 2) [25,26]:

$$\%\ lignin\ in\ surface = \frac{{}^{O}/_{C\ (pulp\ sample)} - {}^{O}/_{C\ (lignin\ free\ pulp)}}{{}^{O}/_{C(lignin)} - {}^{O}/_{C\ (lignin\ free\ pulp)}} \qquad \text{(Eq. 2)}$$

where (O/C) pulp sample is the measured oxygen/carbon atom ratio of BF samples, (O/ C) lignin free pulp is the oxygen/carbon atom ratio without any contamination of a lignin-free (fully-bleached) pulp and (O/C) lignin is the corresponding lignin is the corresponding value for an empirical bamboo lignin from [27]

O/C values were also corrected to take into account contamination of BF surface using (Eq. 3) [28]:

$$\frac{1}{(O/C)\ pulp\ corrected} = \left\{\left[\frac{1+(O/C)cellulose\ measured}{1{,}833}\right] \times \left[\frac{1}{(O/C)pulp\ measured} + 1\right]\right\} \quad \text{(Eq. 3)}$$

where (O/C) pulp corrected is the ratio for the BF sample which takes account of the carbon contamination, (O/C) cellulose measured corresponds to O/C from the lignin free pulp with contamination, where (O/C) pulp measured is the ratio for the BF sample with contamination. Some assumptions were made to establish (Eq. 3): volume chemical composition is assumed uniform, cellulose and hemicellulose are represented by C_6O_5 and lignin bamboo by $C_{8,65}O_{2,35}$ .The (O/C) cellulose measured value was determined by analyzing microcrystalline cellulose (Avicell) paper, in the same conditions as bamboo fibers.

Adhesive forces and roughness at the nanoscale. Adhesives force and nanoscale were measured by AFM using a DIMENSION ICON BRUKER (USA). The roughness was measured in tapping mode using OTESPA probes from Nanoandmore. A PE bead, stuck on a soft cantilever, provided by Novoscan, was used to measure the adhesive force between BF and PE (Fig.S3 in supporting information). PE was used as a substitute for PP because the PE probe is commercially available. It is assumed that PE should behave as PP considering that their surface energy is very close. The spring constant (Kc) was determined by Sader's method. It is equal to 1 N/m [29].

Adhesive forces were determined with approach-retract curves from the cantilever deflection δc, the tip/sample distance D, the rest distance Z between the sample and the cantilever and the sample deformation δd (Fig. 2b) [30, 31]. The baseline was determined by removing the value of the deflection in a non-contact region (Fig 2,a I). The zero separation was obtained from the constant compliance region (Fig 2,a III). All AFM measurements were done in triplicate.

Fig. 2.

2.4 Preparation of fiber mats

Mats of 240 x 880 mm², with a basis weight of 75 ± 5 g/m², were produced using a Mecaform laboratory dynamic sheet former, EP MECA (France), with a jet speed/wire speed ratio equal to 0.6 (Fig. 3). In these conditions, BF are preferentially oriented in the machine direction.

Operating conditions were a flow rate of 1.5 L/min, a drum speed of 1000 rpm, and a pump speed of 600 rpm. Mats were pressed on the wire before removing using a cylindrical roll of 500 g, and then dried at 90.°C for 10 min on a roller calender TECHPAP (France). Densities of the mats are estimated around 0.2 g/cm^3.

Fig. 3.

2.5 Preparation of composites

BF-PP composites were manufactured by film stacking using a thermopress (SAINT ELOI, France) (Fig. 4). The dimensions were set at 180 mm x 180 mm x *1 mm*. Prior to composite manufacturing, PP films were obtained by hot-pressing 8 g of PP pellets at 180.°C and 2 MPa for 60s using the same thermopress. BF mats were dried at 130° C for 4 h to remove moisture. An alternating ply sequence of three BF mats and four PP films was placed between two plates (280mm x 280mm) (Fig. 4). Composite samples were then obtained by hot-pressing using the following operating conditions:

1) Temperature: 200.°C
2) Pre-load: 0.05 MPa
3) Pressure: 0.2 MPa
4) Compression time: 1 min

After hot-pressing, the composites were removed from the press and stored at 23.°C, 50°HR. Neat PP samples, obtained by hot-pressing PP films using the same operating conditions, were also manufactured to serve as reference for mechanical characterization.

Fig. 4.

All BF-PP composites display close properties. Density is around 0.91 ± 0.02 (g/cm^3). The PP film thickness is 0.56 mm and composite thickness is 0.88 ± 0.02 mm. Fiber volume fraction is between 13.% and 14.% for a fiber mass fraction of 23 wt.%. Porosity, calculated by considering a density of 1.5 g/cm^3 for BF, and 0.9 g/cm^3 for the PP is between 8.% and 10.%.

2.6 Composite characterization

Static mechanical analysis. Tensile and flexural tests for neat PP and PP/BF composites were carried out following ASTM D3039 and ASTM D790 standards, respectively, using an Instron Series 5500 universal apparatus (USA). Tensile tests were conducted on 80 mm x 15 mm specimens with a crosshead speed of $2mm \cdot min^{-1}$. For the three-point bending test, the crosshead speed was set at $5mm \cdot min^{-1}$ and the span between two supports was 25 mm. All specimens were conditioned at 23 ± 2 .°C and 50 ± 5.% RH for 24 h prior to mechanical tests. Mean values and standard deviations were calculated from at least 5 samples for each material.

Dynamic mechanical analysis. Dynamic mechanical analysis was performed using a DMA50 manufactured by METRAVIB (France) on 60 mm x 15 mm samples. The frequency was set at 1 Hz with a static and dynamic force of 20 N and 10 N, respectively. Samples were heated from -60 to 120.°C with a heating rate of 2.°C/min.

All mechanical tests were performed on samples in machine direction.

3. Results and discussion

3.2Influence of NaOH treatment on fiber characteristics

Lignin content and morphology of the fibers. To improve the compatibility between fiber and matrix, our strategy consists in keeping a maximum of lignin on the fiber surface. Different experiments were carried out to quantify the residual lignin content and to evaluate the effect of the treatment on the fibers. Results are summarized in Table 1. The bulk lignin content decreases when increasing the soda concentration of the treatment. It decreases from 32 to 21.% for 1.% NaOH concentration, and to 14.% with 30.% NaOH. However, the remaining lignin content between 6.% and 30.% NaOH is close. In fact, at this temperature, NaOH reaches a plateau for delignification due to its action on the α-O-4 linkage of lignin. In fact, these bonds are present only in small proportion in the lignin molecule (4.1.%-4.8.%, [31]), therefore soda treatment is not sufficient for complete delignification [17,33]. The bulk lignin content (X) was used for labelling the samples (BF-X). This referencing will be used for now on in the article. Fiber width remains the same regardless the severity of the treatment, while the length slightly decreases with the 30.% soda treatment due to the partial depolymerization of cellulose [34]. BF

crystallinity index (CI) increases slightly for the weakest soda concentrations, from 46 .% for untreated bamboo to 50.% and 47.% for the 1.% and 6.% NaOH treatments, respectively. This is due to the loss of hemicelluloses, lignin and other non-cellulosic materials, resulting of a less disorder of the organization of the fibers [35]. For the 30.% NaOH treatment, the CI value dramatically decreases to 21.% due to the transformation of cellulose I into cellulose II. Indeed, the cellulose chains have a parallel arrangement in cellulose I, while they have an antiparallel arrangement in cellulose II bringing disorder to the material [36].

Table 1.

The O/C ratio decreases with the severity of the NaOH treatment (Table 1). According to the literature, the main contributors to C-C and C-H bonds are lignin, extractive and contamination caused by the extraction process and by the XPS technique (Fig S2 in supporting information) [25-28]. Based on this assumption, it is possible to calculate the lignin content at the fiber surface using the corrected O/C ratio using (Eq. 3) (see Experimental Section) [28]. Surface lignin content is higher than the bulk lignin content measured by the Klason method (Table 1). Hultén et al. found a surface lignin content between four and five times higher than bulk lignin content [37]. It was attributed to the well-known heterogeneous distribution of cellulose, hemicelluloses and lignin in the fiber wall [37]. The surface lignin content follows the same trends than the bulk content, i.e. it decreases when increasing the severity of the soda treatment. However, a notable difference between the surface lignin content of BF-14 and BF-15 can be observed. Regarding the kinetics of the soda treatment, the lignin removed first is the one available at the surface of BF. Therefore, the difference between the lignin content for BF-15 and BF-14 is higher at the surface than in bulk. Reference measurements of untreated bamboo were performed on strips whereas Gray et al performed measurements on hand-sheets, BF roughness seems to increase with the concentration of NaOH as can be observed in SEM micrographs (Fig. 5). Microfibrils can be evidenced on the surface of treated fibers. BF-14 fibers seem to have swollen. This phenomenon is attributed to the partial mercerization triggered by the high NaOH concentration, as already discussed for XRD experiments. It is also

confirmed by XRD experiments with the presence of the specific peak of the cellulose II à 2 θ =12 and 20 (Fig S1 in supporting information).

Fig. 5

The root mean square (RMS) value of the fiber surface roughness was measured by AFM. Images are shown in Fig 6. Surface roughness first increases with the severity of the soda treatment (72 nm for BF-21 and BF-15, compared to 21 nm for the untreated fiber) but it decreases for BF-14 (37 nm) (Table 2).

Fig.6

The increase in fiber roughness is mainly due to the removal of the small elements and delignification. It reveals microfibrils on the surface of the fibers (Fig 5 b and c) which tends to increase the roughness. Then the increase in roughness reaches a plateau because of mercerization : local fibrillation is reduced [38]

Table 2.

The adhesive force measured by AFM between a PE bead and BF decreases when increasing the severity of the soda treatment (Table 2). This result could be partly explained by the physical properties of bamboo fibers, and in particular by the nanoscale roughness which decreases for BF-14 compared to BF-15 and BF-21. Thus, the specific contact area between the PE bead and the BF-14 fiber is lower than that for BF-15 and BF-21 fibers. The chemical features of the fibers could also partly explain this observation. Since the lignin content on BF surface changes, so does the polarity. This leads to a better compatibility between the less hydrophilic fiber surface and the hydrophobic PE beads. In conclusion, these results confirm that a larger lignin content on the surface increases the adhesion between PE and BF and that was obtained with a soft soda treatment, i.e. 1.% NaOH concentration. Furthermore, the increase of the nano roughness of the fiber seems sufficient to create anchoring of the matrix to the fiber surface. Rozman et al. showed by SEM observation that the interface between a PP matrix and coconut fibers was improved by the addition of lignin, while noting the effect of fiber morphology and roughness [40]. SEM images showed fiber debonding and pull-out in the

composites in the absence of lignin whereas with 30.% lignin, fiber breakage was observed. In our case, we obtained the same results by keeping the lignin naturally present in bamboo.

3.2Mechanical properties of BF-PP composites

The static bending and tensile mechanical properties of the composites are reported in Table 4. Both the bending modulus and strength were improved by the addition of fibers compared to the neat matrix. The flexural modulus increases by 216, 183 and 116.% and the strength by 181, 145 and 115.% compared to neat PP for PP-BF-21, PP-BF-15, and PP-BF-14, respectively.

Table 3.

The elastic modulus and tensile strength of all PP-BF composites are also higher than for neat PP (Table 3). The stiffness and strength were found to be the highest for PP-BF-21 with a 250.% increase in elastic modulus compared to PP. Both PP-BF-21 and PP-BF-15 exhibit very similar elastic modulus values for the same fiber fraction (13-14 .% v/v). However, a higher strength is obtained for PP-BF-21 (53.0 MPa).

The strain at break, on the other hand, decreases following the addition of fibers except for PP-BF-14 which strain at break is almost the same than the one of neat PP. This is probably due to the increase of BF ductility caused by the soda treatment [22].

These results are in contradiction with other reported works that showed that mechanical properties are better for higher NaOH concentrations (~6.%) [40]. However, the authors used different cooking conditions (larger times, lower temperature). Moreover, the PP-BF mechanical properties corresponding to a 1.% NaOH treatment are equivalent or even better than those obtained by other authors for similar or higher fiber fractions, and with stronger chemical treatments. Gu et al. prepared composites by film stacking with a wet-prepared BF mat (40 vol.%) and PP composed of 5.% of maleic anhydride (MAPP). The authors observed a reinforcement of more than 57.% for MAPP-BF composites (2.53 GPa) compared to PP-BF composites (1.61 GPa) [6]. Lee et al. prepared BF reinforced PP composites by extrusion and achieved a reinforcement of 26.% with 30 wt.% of fibers chemically treated with silane to enhance the PP-BF compatibility [16]. Chen et al. manufactured MAPP-BF composites and

obtained with 50 wt.% of BF and 15 wt.% maleic anhydride a tensile modulus between 5 and 6 GPa [41]. The high mechanical properties of PP-BF composites obtained in this study are attributed in part to the soda treatment that leads to elevated BF roughness and less polar surface energy. But it seems, also due to the wet process approach which allows for better properties of the fiber mat by forming homogeneous network bonded by low-energy forces (hydrogen, van der Waals, Coulomb etc…)[42] as in papermaking processes. These results are very encouraging for the development of bio-based composites with high mechanical properties.

The evolution of the storage modulus for neat PP and PP-BF composites as a function of temperature is shown in Fig.7. As expected, the storage modulus for all composites is higher than the one of neat PP in the whole temperature range studied, especially above the glass transition temperature (Tg). Overall, DMA results are consistent with static mechanical experiments: the highest storage modulus corresponds to the less severe NaOH treatment (improvement of 43.% for PP-BF-14 and 245.% for PP-BF-21 at 25.°C, compared to neat PP). The addition of BF strongly decreases the magnitude of the relaxation process (Fig. 8). This observation is directly linked to the decrease of matrix material amount, which is responsible for damping properties, but also to the reduced storage modulus drop in this temperature range. But the diminution is not the same for all composites. This diminution is supposed to be higher for matrix/fiber interphase and interface improved which is the case for PP-BF-21 compared to PP-BF-14. Thus, confirmation is obtained that compatibility between matrix and fibers is improved for higher BF surface lignin content. A plateau is observed starting from 30.°C and onward due to the fiber web. Several relaxation processes of PP can also be observed (Fig 8). The tan δ peak around -20.°C corresponds to β relaxation associated to the Tg of the polymer matrix. Tg decreases with the addition of BF due to a mechanical coupling effect but it seems that this decrease is less noticeable for PP-BF-21 and PP-BF-14 than for PP-BF15 (Table 3).

Fig 7

Fig 8:

3.3 Link between macroscale and microscale analysis

The macroscale mechanical analysis of bamboo fiber reinforced PP laminates shows that the mechanical properties are strongly linked to the severity of the NaOH treatment applied to the fibers. Increasing the NaOH concentration of the treatment results in a decrease in the modulus and strength of the composite in both tensile and bending modes. The storage modulus of the composite also decreases, but the material becomes more ductile with an increase in strain at break. Several microscale parameters could explain this behavior. A first hypothesis is that the decrease in composite performances is associated to BF damaging following the soda treatment. When increasing the NaOH concentration in the solution used for treating the fiber, mercerization occurs, decreasing the crystallinity index, but also the length of the fibers. A severe NaOH treatment damages the fibers, decreases their mechanical properties and thus those of the PP-BF composites. A second hypothesis suggests that the mechanical performances of PP-BF composites are conditioned by firstly the fiber/matrix interactions that are maximized by an elevated BF roughness and secondly by less polar surface energy due to a less polar [43] component i.e. the lignin . A larger roughness enables a stronger mechanical anchoring between matrix and fiber which could explain the better performance of PP-BF-21 and PP-BF-15 compared to PP-BF-14. However, mechanical anchoring can be established only through intimate contact between matrix and fiber, which is permitted by thermodynamics. The lignin surface content strongly changes with the severity of the NaOH treatment: it is higher for a lower NaOH concentration. Moreover, a high surface lignin content and the loss of hydrophilic components like hemicelluloses, which lead a decrease of the water content within the fibers in case of the soft soda treatment. means a less polar BF surface energy, thus a better compatibility with the fully dispersive PP matrix. In case of severe treatment, even if the content of hemicellulose decreases the accessibility of hydroxyl groups of the cellulose increases and so the water content in BF too (data available in supporting information). This could explain the better properties of PP-BF-21 compared PP-BF-15 and PP-BF-14. This explanation is consistent

with AFM force measurement indicating higher adhesion forces between PE and BF-21 (Table 2). It is also consistent with the decrease in tan δ peak magnitude for PP-BF-21 (Fig. 7). Overall, the best mechanical performances were obtained for the highest measured adhesive forces between BF and PE, for the roughest BF, showing the highest bulk and surface lignin content, which corresponds to fibers prepared with a 1.% soda concentration. This study also confirms the possibility of explaining large-scale behavior of materials by small-scale analyses.

4. Conclusions

In this study, laminate composites composed of BF and PP were manufactured and characterized. Good mechanical performances were obtained. The best mechanical properties correspond to a 1.% NaOH chemical treatment for the preparation of BF. It leads to an increase in Young's modulus of 250.% and an increase in strength of 188.% compared to neat PP. This analysis confirms previous studies that this soda concentration is sufficient to individualize fibers, to obtain good mat, and good composites. Furthermore, this treatment is quite safe and cheap compared to other chemical treatments. The wet laid process used for manufacturing the mat seems to be a good way to obtain reproducible and good quality materials. The multiscale study by AFM and XPS confirms the macroscale study by static and dynamic mechanical analysis. By increasing the roughness of the fibers and maintaining a large amount of lignin on their surface, the adhesion between matrix and fibers is improved, which enhances the compatibilization between matrix and fibers and thus the mechanical properties of the composites. The link between the microscale and the macroscale phenomena was proven effective. This type of approach could be a solution for predicting the behavior of composites from microscale characterizations.

Acknowledgements

LGP2 is part of the LabEx Tec 21 (Investissements d'Avenir - grant agreement n°ANR-11-LABX-0030) and of PolyNat Carnot Institute (Investissements d'Avenir - grant agreement n° ANR-16-CARN-0025-01). This research was made possible thanks to the facilities of the TekLiCell platform funded by the Région Rhône-Alpes (ERDF: European regional

development fund) and the LabEx CEMAM (Investissements d'Avenir, grant agreement #ANR-10-LABX-44-01). The authors gratefully acknowledge Research and Researchers for Industries Scholarship (Grant No. PHD 60I0039) and Charoen Triphop Limited Partnership for their financial support during the research. The authors also thank Thierry Encinas and Stephane Coindeau (CMTC, Grenoble) for the XRD acquisition, and Bertine Khelifi (LGP2) for SEM images.

Data availability

All data generated or analysed during this study are included in this published article [and its supplementary information files].

Conflict of Interest

The authors declare that they have no known competing financial interests or personal relationships that could have appeared to influence the work reported in this paper.

References

References

[1] Gholampour A, Ozbakkaloglu T. A review of natural fiber composites: properties, modification and processing techniques, characterization, applications. J Mater Sci 2020; 55(3):829-892.

[2] Faruk O, Bledzki AK, Fink H-P, Sain M. 2012. Biocomposites reinforced with natural fibers: 2000–2010. Prog Polym Sci 2012;37(11):1552-1596.

[3] Ramamoorthy SK, Skrifvars M, Persson A. A review of natural fbers used in biocomposites: plant, animal and regenerated cellulose fibers. Polym Rev 2015;55(1):107-162.

[4] Hasan KMF, Faridul, Horváth PG, Bak M, Alpár T. A state-of-the-art review on coir fiber-reinforced biocomposites. RSC Adv 2021;11(18):10548-10571.

[5] Al-Oqla FM, Salit MS. Materials Selection for Natural Fiber Composites. Woodhead Publishing: Elsevier, 2017.

[6] Gu F, Zheng Y, Zhang W, Yao X, Pan D, Wong ASM, Guo J, Hall P, Sharmin N. Can bamboo fibers be an alternative to flax fibers as materials for plastic reinforcement? A comparative life cycle study on polypropylene/flax/bamboo laminates. Ind Crops Prod 2018;121:372-87.

[7] Jawaid M, Rangappa SM, Siengchin S, Bamboo Fiber Composites: Processing, Properties and Applications. Springer Verlag: Singapore; 1st ed., 2021.

[8] https://www.selinawamucii.com/insights/prices/china/bamboo/.

[9] Koronis G, Silva A. Green Composites for Automotive Applications. Woodhead Publishing: Elsevier, 2019.

[10] Yu Y, Yan, Tian G, Wang H, Fei B, Wang G. Mechanical characterization of single bamboo fibers with nanoindentation and microtensile technique. Holzforschung 2011:65(1):113-119.

[11] Abdul Khalil HPS, Bhat IUH, Jawaid M, Zaidon A, Hermawan D, Hadi YS. Bamboo fiber reinforced biocomposites: a review. Mater Des 2012;42:353-368.

[12] Doineau E, Cathala B, Benezet J-C, Bras J, Le Moigne N. Development of bio-inspired hierarchical fibers to tailor the fiber/matrix interphase in (bio)composites. Polymers 2021;13(5): 804.

[13] Lee K-Y, Bharadia P, Blaker JJ, Bismarck A. Short sisal fiber reinforced bacterial cellulose polylactide nanocomposites using hairy sisal fibers as reinforcement. **Compos Part A Appl Sci Manuf** 2012;43(11):2065-2074.

[14] Qiu W, Zhang F, Endo T, Hirotsu T. 2005. Isocyanate as a compatibilizing agent on the properties of highly crystalline cellulose/polypropylene composites. J Mater 2005;40:3607-3614.

[15] Espino-Pérez E, Domenek S, Belgacem N, Sillard C, Bras J. Green process for chemical functionalization of nanocellulose with carboxylic acids. Biomacromolecules 2014;15(12):4551-4560.

[16] Lee S-Y, Chun S-J, Doh G-H, Kang I-A, Lee S, Paik K-H. 2009. Influence of chemical modification and filler loading on fundamental properties of bamboo fibers reinforced polypropylene composites. J Compos Mater 2009;43(15):1639-1657.

[17] Kondo R, Sarkanen KV. Kinetics of lignin and hemicellulose dissolution during the initial stage of alkaline pulping. Holzforschung 1984;38(1):31-36.

[18] Khan Z, Yousif BF, Islam M. 2017. Fracture behaviour of bamboo fiber reinforced epoxy composites. Compos B Eng 2017;116:186-199.

[19] Martijanti M, Juwono AL, Sutarno S. Investigation of characteristics of bamboo fiber for composite structures. IOP Conf Ser Mater Sci Eng 2020;850:012028.

[20] Chen H, Cheng H, Wang G, Yu Z, Shi SQ. Tensile properties of bamboo in different sizes. J Wood Sci 2015;61:552-561.

[21] Das M, Chakraborty D. Evaluation of improvement of physical and mechanical properties of bamboo fibers due to alkali treatment. J Appl Polym Sci 2008;107(1):522-527.

[22] Chen H, Yu Y, Zhong T, Wu Y, Li Y, Wu Z, Fei B. Effect of alkali treatment on microstructure and mechanical properties of individual bamboo fibers. Cellulose 2017;24(1),333-347.

[23] Ahvenainen P, Kontro I, Svedström K. 2016. Comparison of sample crystallinity determination methods by X-ray diffraction for challenging cellulose I materials. Cellulose 2016;23(2):1073-1086.

[24] Park S, O Baker J, Himmel ME, Parilla PA, Johnson DK. Cellulose crystallinity index: measurement techniques and their impact on interpreting cellulase performance. Biotechnol Biofuels 2010;3:10.

[25] Johansson LS, Campbell JM, Koljonen K, Stenius P. 1999. Evaluation of surface lignin on cellulose fibers with XPS. Appl Surf Sci 1999;144-145:92-95.

[26] Laine J, Stenius P, Carlsson G, Ström G. 1994. Surface characterization of unbleached kraft pulps by meansof ESCA. Cellulose 1994;1(2):145-60

[27] Wen, J.- L., Sun, S.-L. , Xue , B.-L., & Sun, R.-C. (2012).Quantitative structural characterization of the lignins from the stem and pith of bamboo(Phyllostachys pubescens *).* Holzforschung 2013; 67(6): 613–627.

[28] Gray D, Weller GM, Ulkem N, Lejeune A. Composition of lignocellulosic surfaces: comments on the interpretation of XPS spectra. Cellulose 2010;17(1):117-124.

[29] Sader JE, Chon JWM, Mulvaney P. Calibration of rectangular atomic force microscope cantilevers. Rev Sci Instrum 1999;70(10):3967-3969.

[30] Ralston J, Larson I, Rutland MW, Feiler AA, Kleijn M. Atomic force microscopy and direct surface force measurements (IUPAC Technical Report). Pure Appl Chem 2005;77(12): 2149-2170.

[31] Cappella B, Dietler G. Force-distance curves by atomic force microscopy. Surf Sci Rep 1999;34(1-3):1-104.

[32] Wen, J.-L., Sun, S.-L., Xue, B.-L., & Sun, R.-C. Quantitative structural characterization of the lignins from the stem and pith of bamboo (Phyllostachys pubescens). Holzforschung, (2013) 67(6), 613-627.

[33] Gierer J. Chemical aspects of kraft pulping. Wood Sci Technol 1980;14(4):241-266.

[34] Isogai A, Atalla RH. Dissolution of cellulose in aqueous NaOH solutions. Cellulose 1998;5(4):309-319.

[35] Das M, Chakraborty D. Influence of alkali treatment on fine structure. J Appl Polym Sci 2006;102:5050-5056.

[36] El Oudiani A, Chaabouni Y, Msahli S, Sakli F. Crystal transition from cellulose I to cII in NaOH treated *Agave americana* L. fiber. Carbohydr Polym 2011;86(3):1221-1229.

[37] Hultén AH, Basta J, Larsson P, Ernstsson M. Comparison of different XPS methods for fiber surface analysis. Holzforschung 2006;60(1):14-19.

[38] Eronen P, Österberg M, Jääskeläinen A-S. Effect of alkaline treatment on cellulose supramolecular structure studied with combined confocal Raman spectroscopy and atomic force microscopy. Cellulose 2009;16(2):167-178.

[39] Chen H, Zhang W, Wang X, Wang H, Wu Y, Zhong T, Fei B. Effect of alkali treatment on wettability and thermal stability of individual bamboo fibers. J Wood Sci 2018;64(4):398-405.

[40] Rozman HD, Tan KW, Kumar RN, Abubakar A, Mohd Ishak ZA, Ismail H. The effect of lignin as a compatibilizer on the physical properties of coconut fiber-polypropylene composites. Eur Polym J 2000;36(7):1483-1494.

[41] Zhang K, Wang F, Liang W, Wang Z, Duan Z, Yang B. Thermal and mechanical properties of bamboo fiber reinforced epoxy composites. Polymers 2018;10(6):608.

[412] Chen X, Guo Q, Mi Y. Bamboo fiber-reinforced polypropylene composites: a study of the mechanical properties. J Appl Polym Sci 1998;69(10):1891-1899.

[43] Hirn, U., & Schennach, R. (2015). Comprehensive analysis of individual pulp fiber bonds quantifies the mechanisms of fiber bonding in paper. Scientific reports, 5(1), 1-9.

[44] Winter, A., Andorfer, L., Herzele, S., Zimmermann, T., Saake, B., Edler, M., Griesser, T., Konnerth, J., & Gindl-Altmutter, W. (2017). Reduced polarity and improved dispersion of microfibrillated cellulose in poly(lactic-acid) provided by residual lignin and hemicellulose. J Mater Sci, 52(1), 60-72.

Figures

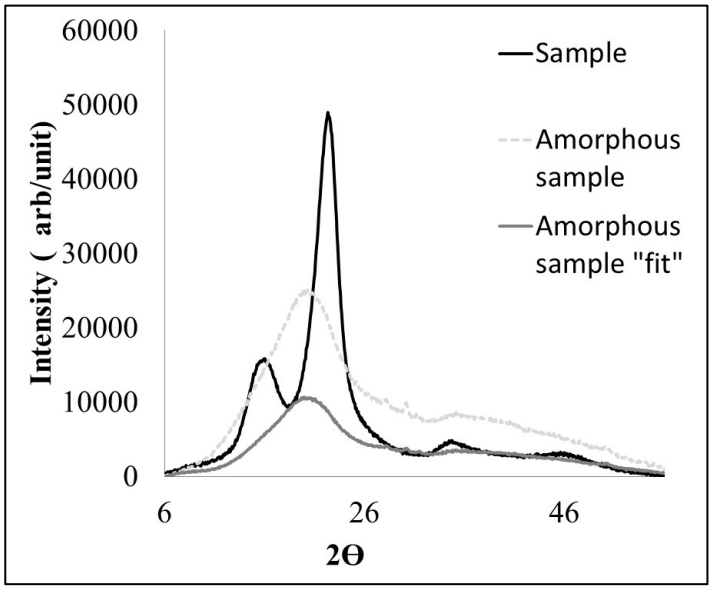

Fig. 1. Crystallinity index measurement: amorphous fitting subtraction on bamboo fiber sample.

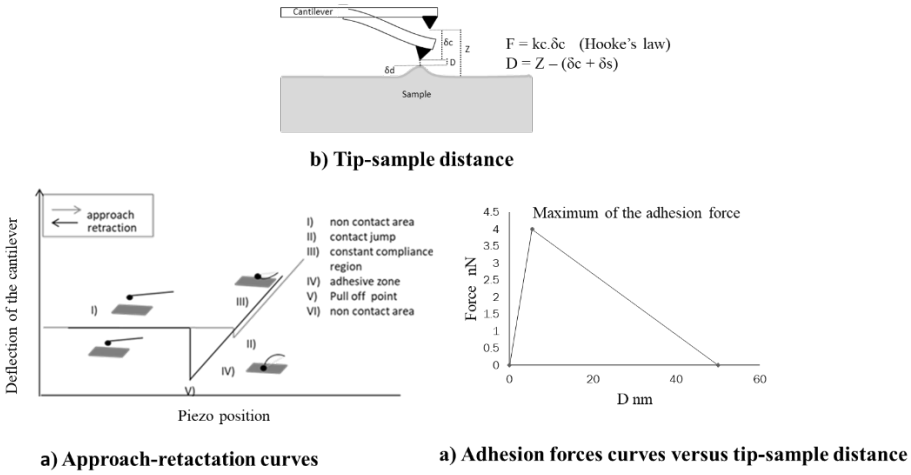

Fig. 2. Principle of the adhesion measurement by AFM. a) the approach/ retraction curves b) the tip/surface distance calculation, c) the adhesion force versus distance after calibrations.

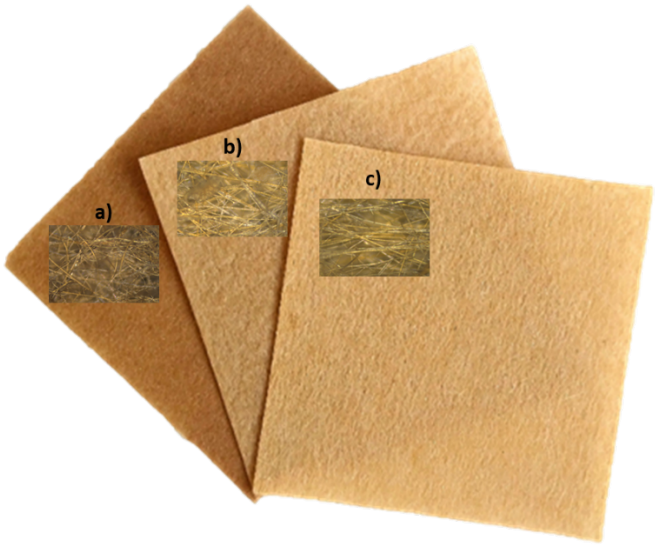

Fig. 3. Pictures and optical microscopy images (x10) of BF mats treated with a) 30%, b) 6% and c) 1% NaOH concentration

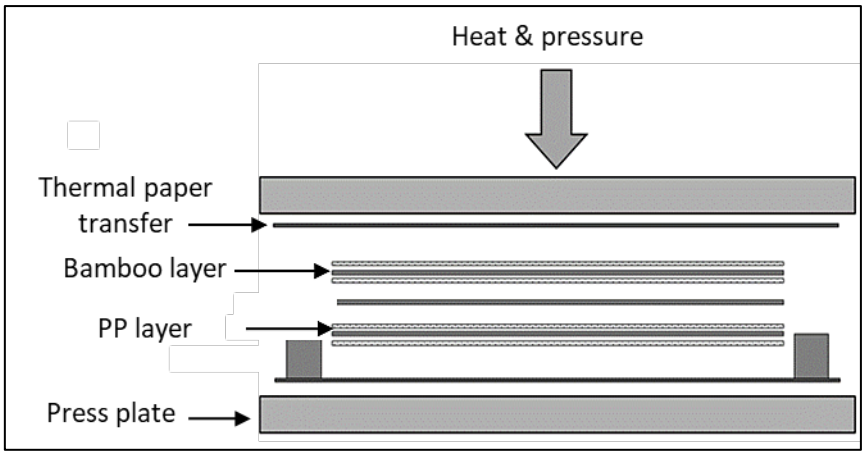

Fig. 4. Composite manufacturing process.

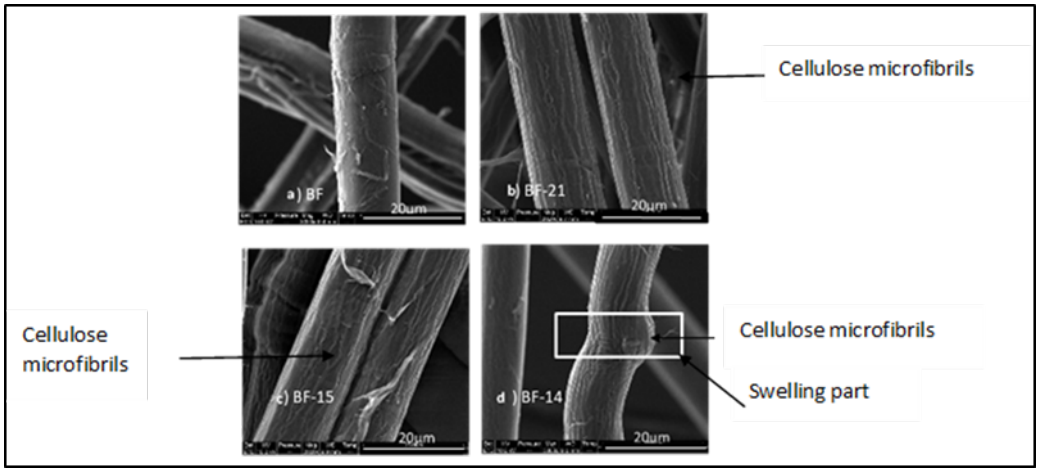

Fig. 5. SEM images of fibers treated with different NaOH concentrations a) BF b) BF-21 c) BF-15 and d) BF-14.

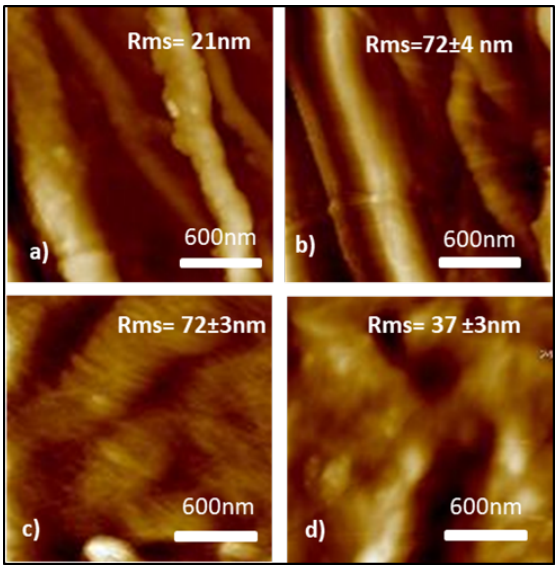

Fig.6 AFM images of fibers treated with different NaOH concentrations a) BF b) BF-21 c) BF-15 and d) BF-14.

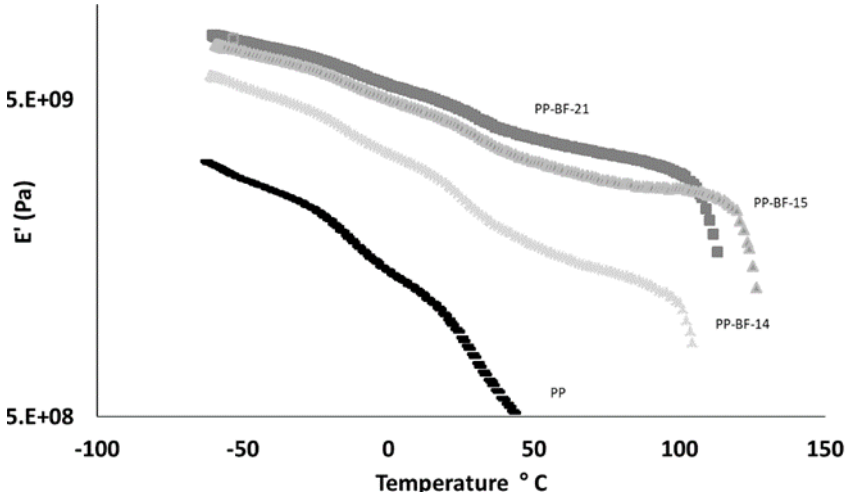

Fig 7: Evolution of the storage modulus for PP-BF composites and neat PP as a function of temperature for PP (-), PP-BF-14 ( ), PP-BF-15 (▲), and PP-BF-21 ( )

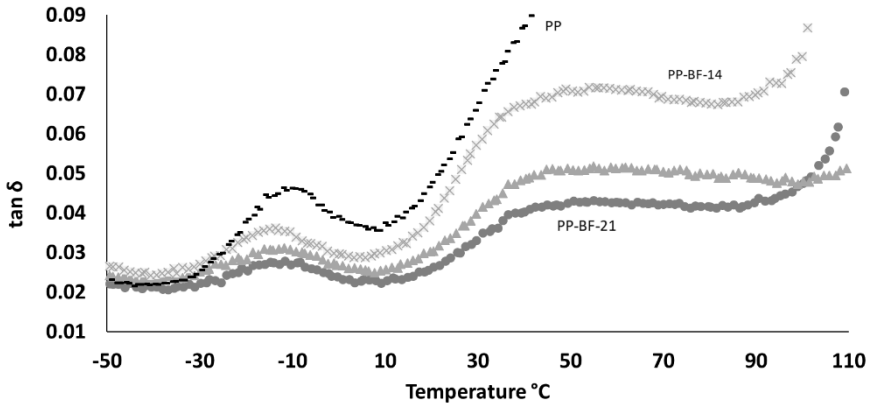

Fig 8: Evolution of tan δ for PP-BF composites and neat PP as a function of temperature for PP (-), PP-BF-14 ( ), PP-BF-15 (▲), and PP-BF-21 ( )